Journal of Organometallic Chemistry, 390 (1990) 227–235
Elsevier Sequoia S.A., Lausanne – Printed in The Netherlands
JOM 20777

Cryptates from cryptands containing the ferrocene unit. Determination of equilibria stoicheiometries and stability constants

C. Dennis Hall *, Ian P. Danks and Nelson W. Sharpe
Department of Chemistry, King's College, University of London, Strand, London WC2R 2LS (U.K.)
(Received January 17th, 1990)

Abstract

Electronic absorption spectroscopy has been used to study the host-guest interaction of a series of ferrocene-containing cryptands and macrocycles with a range of metal cations (M^{n+} = Be^{2+}, Mg^{2+}, Ca^{2+}, Sr^{2+}, Ba^{2+}, Eu^{3+}, Tb^{3+}, Dy^{3+}, Mn^{2+} and Zn^{2+}) in acetonitrile solutions. Complexation results in a bathochromic shift of the lowest energy ferrocene-centred *d–d* transitions. Host-guest complexation stoicheiometries have been determined. The stability constants for these equilibria have been evaluated.

Introduction

Over recent years [1–3] we have synthesised a range of ferrocene-containing cryptands and macrocycles **1–5** (the structures of which are shown in Fig. 1), together with one acyclic bis-diamide **6**. These compounds have been observed to complex metal cations in acetonitrile solution. The complexation causes shifts in the ferrocene-centred redox couple [4] and marked changes in the ^{13}C and ^{1}H NMR spectra of the host macrocycle [5]. For complexes of **1** with Group II cations, ^{13}C NMR studies (at equimolar concentrations of ca. 10^{-2} *M*) reveal the presence of both 2/1 and 1/1 host-guest complexes, with the 1/1 stoicheiometry favoured at lower concentrations and higher temperatures.

Complexation of the guest metal cation also causes the broad ferrocene-centred absorption band at ca. 452 nm to shift to longer wavelength with an increase in the extinction coefficient (see Fig. 2). Monitoring the changes in the visible absorption spectrum, upon incremental addition of the metal cation, from the free ligand host to the host-guest metal complex permits the determination of both the complexation stoicheiometries and the equilibrium constants for these host-guest interactions.

Experimental

Absorption spectra were recorded on a Unicam SP1700 Ultraviolet Spectrophotometer with the cells thermostatted at $30 \pm 1°C$.

The alkaline earth metal cation solutions were prepared from their perchlorates which were dried at 120 °C (1 mmHg, 3 h). Spectroscopic grade acetonitrile was used throughout, dried by the usual procedures, and stored under nitrogen over 4Å molecular sieves. The water content of these solutions was determined with a Mitsubishi water meter and adjusted to 2.25 mol of water per mol of metal ion. For the transition metals, the solutions were prepared from their tetrafluoroborate-acetonitrile complexes [6], whose MeCN content was determined by calibrated NMR methods. Rare earth perchlorate hexahydrates $\{Ln(ClO_4)_3 \cdot 6H_2O$ (Ln = Eu, Tb, Dy) were used as purchased (Ventron-Alfa Products). Time resolved luminescence measurements confirmed that the species in solution was the solvated lanthanide hexa-aquo ion.

For these absorption experiments the concentration of host macrocycle was in the range 2×10^{-3} *M*, which is an order of magnitude less than that used in our previous NMR studies [5]. At these lower concentrations 1/1 host-guest complexes are favoured.

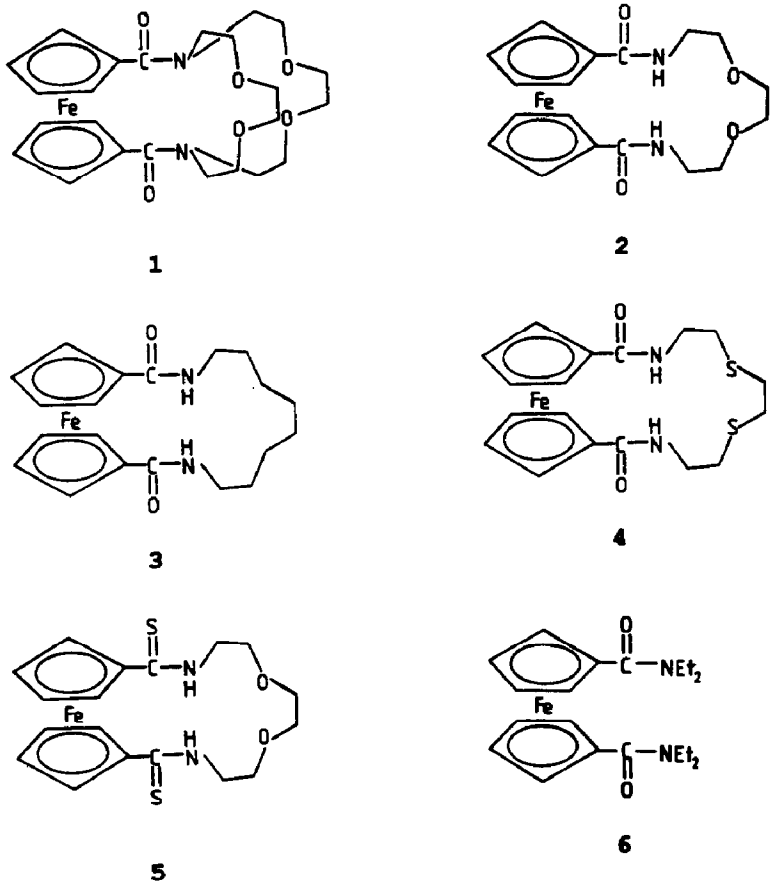

Fig. 1. Ferrocene containing macrocycles.

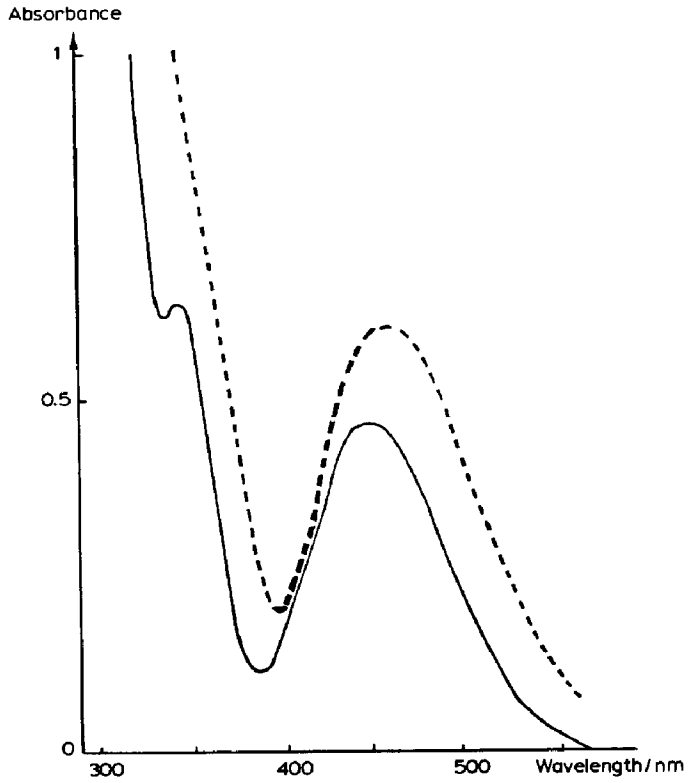

Fig. 2. Absorption spectrum of **1** (full line) and of the cryptate (Ca^{2+} : (**1**)) (dotted line). These typify the UV/vis. spectra for the ferrocene-containing cryptand, macrocycles and bis-diamide **1–6** (full line), and that of their complexes with metal cations (dotted line).

Compounds **1**, **2** and **6** were prepared as described previously [1,2]. Compound **3** was synthesised from 1,8-diaminooctane by a method analogous to that used for **2**. Compounds **4** and **5** have not been reported previously.

1,1′(4,7-Dithia-1,10-diazadecane-1,10-diyldicarbonyl)ferrocene (4)

A solution of 1,1′-bis(chlorocarbonyl)ferrocene (0.50 g) in toluene (125 ml) and a mixture of 1,8-diamino-3,6-dithiaoctane (0.28 g) and triethylamine (1.1 ml) in toluene (125 ml) were added dropwise separately and simultaneously during 2 h to vigorously stirred toluene (100 ml, 70 °C) under nitrogen. The solution was stirred at 70 °C for a further 4 h and allowed to stand at room temperature for 12 h. The precipitate was removed by filtration and the orange solution evaporated to dryness under reduced pressure. The residue was chromatographed on alumina with dichloromethane (99%)/methanol (1%) as eluent. The orange band collected was evaporated to dryness. Trituration with diethyl ether yielded the product **4** (orange powder, 0.18 g, 27%, dec. > 175 °C). Found: C, 52.33; H, 5.10; N, 6.59. $C_{18}H_{22}N_2O_2S_2Fe$ calcd.: C, 51.67; H, 5.31; N, 6.70%. M^+, 418. δ (ppm), 2% CD_3OD in CD_2Cl_2, 2.90 (t, 4H, *J* 5 Hz), 2.99 (s, 4H), 3.67 (dt, 4H, *J* 5, 6 Hz), 4.34 (dd, 4H, *J* 2, 2 Hz), 4.66 (dd, 4H, *J* 2, 2 Hz), 6.76 (t {broad}, 2H, *J* 6 Hz).

1,1'-(4,7-Dioxa-1,10-diazadecane-1,10-diyldithiocarbonyl)ferrocene (5)

Lawesson's reagent (60 ml) was added to a stirred solution of **2** (50 mg) in dimethoxyethane (3 ml, 60 °C). The solution was stirred at 60 °C for 5 h and then allowed to cool and added to water (20 ml). After extraction with dichloromethane (3 × 25 ml) the extract was washed with water (3 × 50 ml), dried over magnesium sulphate, filtered, and evaporated to dryness under reduced pressure. The residue was chromatographed on silica with dichloromethane (99%)/methanol (1%) as eluent. The collected orange band was evaporated to yield a red-brown oil, which crystallised on standing and was triturated with diethyl ether to yield the product **5** (orange-brown powder, 43 mg, 85%, m.p. 123 °C). Found: C, 52.05; H, 5.39; N, 6.19. $C_{18}H_{22}N_2O_2S_2Fe$ calcd.: C, 51.67; H, 5.31; N, 6.70%. M^+, 418. δ (ppm), $CDCl_3$, 3.76 (s, 4H), 3.85 (t, 4H, *J* 5 Hz), 4.04 (dt, 4H, *J* 5, 5 Hz), 4.56 (dd, 4H, *J* 2, 2 Hz), 4.66 (dd, 4H, *J* 2, 2 Hz), 7.09 (t {broad}, 2H, *J* 5 Hz).

Results

Incremental addition of metal cation to a solution of **1** (λ_{max} 452 nm) caused a bathochromic shift in λ_{max} up to a limiting value at which point the equilibrium is fully in favour of the complexed species, and further addition of metal cation is therefore in excess. These limiting values of λ_{max} (in nm, errors ±2) for each cation are as follows, with the extinction coefficients (in $mol^{-1}\ dm^3\ cm^{-1}$) in parentheses: Be^{2+} 465 (380), Mg^{2+} 465 (320), Ca^{2+} 465 (340), Sr^{2+} 462 (320), Ba^{2+} 465 (260), Eu^{3+} 477 (390), Tb^{3+} 478 (380), Dy^{3+} 478 (380), Mn^{2+} 462 (320) and Zn^{2+} 464 (340). The trivalent cations were observed to cause larger bathochromic shifts, and in general there was a trend toward higher extinction coefficients of the complex for metal cations with the greater ratio of charge to ionic radius. This trend toward higher extinction coefficients for the complexes formed by the more charge dense metal cations was also observed for the host-guest complexes of **2–6**. The magnitude of the bathochromic shift upon complexation of **1–6** with Group II metal cations seems to be independent of cation charge density, and this shift also shows no correlation with the derived equilibrium constants.

The increase in absorbance at λ_{max} for the complex (Ca^{2+} : (**1**)) upon incremental addition of Ca^{2+} to a solution of **1** is given in Table 1. The data are illustrated in Fig. 3a. It is clear that the progressive increase in absorbance intercepts the limiting 'infinity' absorbance at molar equivilance of Ca^{2+} to **1**. Therefore the complexation stoicheiometry for the complex (Ca^{2+} : (**1**)) is 1/1 as represented by eq. 1

$$Ca^{2+} + \mathbf{1} \overset{K_1}{\rightleftharpoons} (Ca^{2+} : (\mathbf{1})) \quad (1)$$

The equilibrium constant was calculated by a least squares fitting program based on that for solutions to quadratic equations [7] to yield a value for the bimolecular equilibrium constant, K_1, of 13900 $mol^{-1}\ dm^3$.

Table 1 also gives absorption data for the incremental addition of Ca^{2+} to the macrocycle **2**, which is illustrated in Fig. 3b. In this case, the increasing gradient of the low [Ca^{2+}] region intercepts the limiting 'infinity' absorbance of the complex at 50% mole ratio of Ca^{2+} to **2**. Therefore the complexation stoicheiometry is 2/1 and the equilibrium is that described by eq. 2.

$$Ca^{2+} + 2\,\mathbf{2} \overset{K_2}{\rightleftharpoons} (Ca^{2+} : (\mathbf{2})_2) \quad (2)$$

Table 1

Absorption data at complex λ_{max} for solutions of **1** and **2** (both 2×10^{-3} M) upon incremental mole percent addition of Ca^{2+}

% of Ca^{2+} to **1**	A_{465}	% of Ca^{2+} to **2**	A_{458}
0	0.480	0	0.430
8.3	0.496	8.3	0.446
16.7	0.512	16.7	0.462
25.0	0.527	25.0	0.475
33.0	0.543	33.0	0.486
41.7	0.558	41.7	0.494
50.0	0.573	50.0	0.500
58.3	0.587	58.3	0.504
66.7	0.601	66.7	0.507
75.0	0.614	75.0	0.510
83.3	0.625	83.3	0.512
91.7	0.636	100.0	0.515
100.0	0.644	116.7	0.518
108.3	0.650	150.0	0.521
116.7	0.656	200.0	0.524
125.0	0.659	250.0	0.526
133.3	0.662	300.0	0.527
141.7	0.664		
150.0	0.666		
160.0	0.666		
180.0	0.667		
200.0	0.667		
250.0	0.667		
300.0	0.668		

The equilibrium constant was evaluated by use of a least squares fitting program based on that for solutions to cubic equations [7] to yield a value for the termolecular equilibrium constant, K_2, of 3.2×10^6 mol^{-2} dm^6.

Table 2 collects together all the equilibrium stoicheiometries and equilibrium constants for the range of complexes studied. In addition to these, complexation of Cu^{2+} and Fe^{3+} cations was observed, which resulted in oxidation of the ferrocene-containing macrocycle to yield the ferrocenium analogue, prior to subsequent decomposition.

The interaction of Dy^{3+} with **1** provides an illustration of the stepwise nature of successive equilibria. Table 3 gives the absorption data for a solution of **1** upon incremental addition of Dy^{3+} measured at 452 and 478 nm. These data are illustrated in Fig. 4a and 4b. In Fig. 4a monitoring absorption changes at 452 nm indicates a complexation stoicheiometry of $(Dy^{3+}:(\mathbf{1})_2)$, with an equilibrium constant $K_2 = 33\times10^6$ mol^{-2} dm^6. At this monitoring wavelength, the λ_{max} for the free uncoordinated **1**, there is an increase in absorbance which is proportional to the formation of the $(Dy^{3+}:(\mathbf{1})_2)$ complex. The absorbance reaches a steady value at a mole ratio 2/1 of **1** to Dy^{3+}, and thereafter the addition of more Dy^{3+} drives the equilibria towards the 1/1 complex without a significant change in absorbance at 452 nm. Figure 4b shows the results of monitoring of the complexation equilibria at 478 nm, which is λ_{max} for the complexation stoicheiometry $(Dy^{3+}:(\mathbf{1}))$, and the plot reveals two gradients and two intercepts with the limiting 'infinity' absorbance.

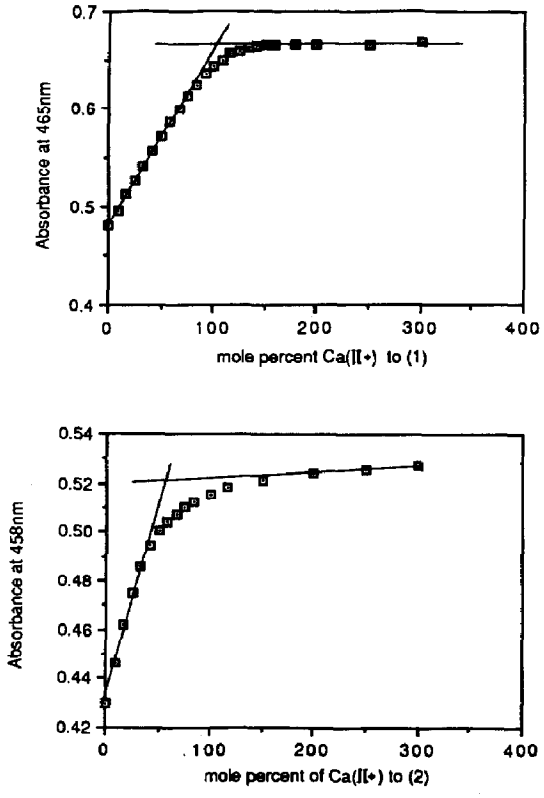

Fig. 3. Plots of absorbance versus mole percent of metal cation to ferrocene macrocycle; (a) for Ca^{2+} with **1**, and (b) for Ca^{2+} with **2**. Data from Table 1.

The equilibria involved are depicted in Scheme 1. In the regime from 0–40% mole ratio, the data shown in Fig. 4a analyse for K_2. In Fig. 4b, the data in the regime 60–100% mole ratio, which intercept the limiting 'infinity' absorbance at 100% mole ratio, may be used to give a value for K_1 of 32×10^3 mol^{-1} dm^3. The third equilibrium constant, K_3, is then calculated to be 1×10^3 mol^{-1} dm^3, since $K_2 = K_1 \times K_3$.

Similar data for the complexation of Tb^{3+} to **1** have been obtained. However in this case, since $(Tb^{3+} : (\mathbf{1}))$ and $(Tb^{3+} : (\mathbf{1})_2)$ have indistinguishable λ_{max} values and

Table 2

$\log_{10} K_x$ ($x = 1$ or 2) for $(M^{2+} : (L)_x)$ in MeCN

Macrocyclic host, L	Be^{2+}	Mg^{2+}	Ca^{2+}	Sr^{2+}	Ba^{2+}	$(M^{2+} : (L)_x)$ stoicheiometry
1	4.1	3.5	4.2	4.2	4.5	1/1
2	5.9	6.6	6.5	–	6.0	1/2
3	–	6.2	7.0	5.8	–	1/2
4	–	5.9	6.9	6.4	6.7	1/2
5	No complex formation					
6	–	5.8	7.2	6.3	6.1	1/2

[a] For **4**, the solvent used was $MeCN/CHCl_3$ (1/1). [b] $Mn^{2+}(BF_4^-)_2$ and $Zn^{2+}(BF^-)_2$ gave similar complexes with K_x values approximately one order of magnitude lower.

Table 3

Absorption data at 478 and 452 nm for solutions of **1** (at 2×10^{-3} *M*) upon incremental mole percent addition of Dy^{3+}

% of Dy^{3+} to **1**	A_{478}	A_{452}
0	0.393	0.480
3.0	0.416	0.494
5.6	0.427	0.491
11.1	0.469	0.532
16.7	0.524	0.554
24.3	0.584	0.593
37.5	0.651	0.635
46.1	0.700	0.667
56.7	0.724	0.682
67.6	0.738	0.686
78.2	0.747	0.682
91.4	0.758	0.680
142.0	0.772	0.693
192.6	0.776	0.691
243.3	0.777	0.690
293.9	0.779	0.691

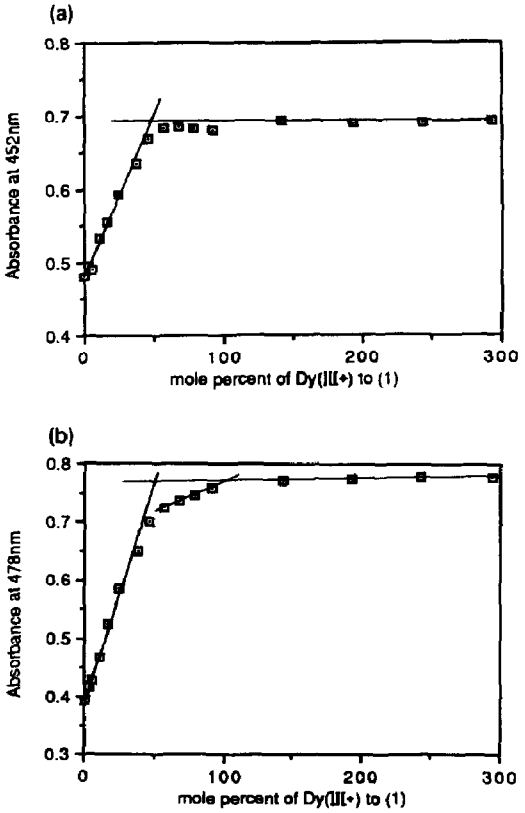

Fig. 4. Plots of absorbance versus mole percent of Dy^{3+} to **1**; (a) monitored at 452 nm, and (b) monitored at 478 nm. Data from Table 2.

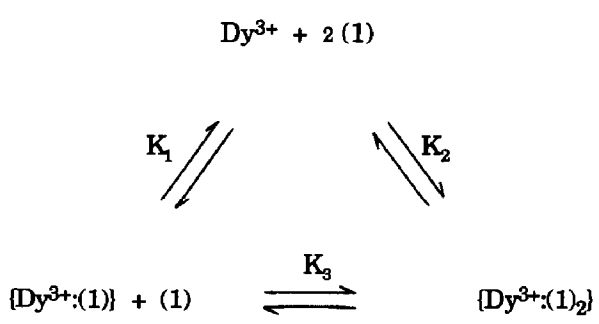

Scheme 1

extinction coefficients, evaluation of both stability constants is precluded. This feature was noted in our previous report on the electrochemistry of these systems [4].

Discussion and conclusions

Several conclusions as to the nature of the interaction in solution of metal cations with the range of ferrocene-containing structures **1**–**6** may be drawn, as examination of Table 2 reveals. Most importantly, the principal functionality responsible for metal cation coordination is the carbonyl group of the amide. This is demonstrated conclusively by the fact that **5** is incapable of complex formation, owing to replacement of carbonyl by thiocarbonyl functionality. Therefore, O-atom donor coordination to the metal cation is crucial. Furthermore, the coordinating role played by the heterocyclic bridges is clearly secondary, as demonstrated by the data for **6**. This acyclic bis-diamide does not possess heterocyclic bridges, and yet exhibits values of K_2 comparable to those for structures with heterocyclic bridge functionality. Also, the comparability of the K_2 values for **4** and **2** suggests that replacement of the oxa-ether by the thia-ether functionality within the heterocyclic bridges results in only small changes in the ability of the molecules to coordinate metal cations. Indeed, for **3**, which contains no heteroatom within the polymethylene bridge between the amide functions, values of K_2 are comparable with those for **2** and **4**, confirming the dominant role of the carbonyl groups in coordination of the metal cation. Although the dithiocarbonyl macrocycle **5** does not form complexes with the metal cations listed in Table 2, it does interact with the 'soft' metal cations, Ag^+ and Hg^{2+}. Finally, there appears to be little or no selectivity for a particular dication, either as 1/1 or 1/2, $(M^{2+}:(L)_x)$, complexes. This is as expected if the amide carbonyl groups are the principal coordinating functions. It contrasts, however, with the extraction experiments reported in our first communication [8], and suggests that the results obtained by extraction of picrate salts into dichloromethane need further examination.

At these concentrations, the coordination stoicheiometries are seen to be 1/2 for the complexes $(M^{2+}:(L)_x)$ formed except for **L** = **1**, for which a 1/1 stoicheiometry is observed. Our previous NMR studies [5] have shown the complex equilibria to be shifted in favour of $(M^{2+}:(\mathbf{1})_2)$ at higher concentrations and lower temperatures. However at the concentration used in this study it is $(M^{2+}:(\mathbf{1}))$ which is favoured. For **1**, the macrocyclic structure comprises two bridges, and it appears that this

second bridge results in steric hindrance which inhibits formation of the 2/1 host-guest complex ($M^{n+}:(L)_2$).

Bridged ferrocenes have been observed previously to exhibit blue shifts [9] and red shifts [10] in the 440 nm *d–d* absorption of ferrocene. These latter bathochromic shifts have been attributed to the interplanar tilting of the cyclopentadienyl rings of the bridged ferrocene unit [11]. The crystal structure of **1** is known [12] and shows the cyclopentadienyl rings to be slightly tilted, with an interplanar dihedral angle of 0.4°. The structure also reveals an inter-ring twist angle of 6.4° from eclipsed for the ferrocene moiety.

For ferrocene the absorption band centred at 440 nm has been shown to be an envelope consisting of two spin-allowed ligand field transitions [13]. Theoretical models [14,15] led to the suggested assignments for the particular transitions involved. Our previous NMR studies [5] suggest that for **1**, upon complexation of the metal cation, the cyclopentadienyl rings become eclipsed, i.e. there is local D_{5h} symmetry for the ferrocene unit. Under D_{5h}, the degeneracy of both the e_2' (HOMO) and the e_1'' (LUMO) orbital energy levels is restored (they are split in uncomplexed **1**), and therefore the wavelength of the visible transitions between these levels change. This may be one possible explanation for the origin of the bathochromic shift of the band centred at ca. 450 nm for the ferrocene-containing macrocycles upon complexation of metal cations.

Acknowledgement

Thanks are extended to the S.E.R.C. (I.P.D.) and RTZ Chemicals Ltd. (N.W.S.) for financial support.

References

1 P.J. Hammond, A.P. Bell and C.D. Hall, J. Chem. Soc. Perkin Trans., (1983) 707.
2 P.J. Hammond, P.D. Beer, C. Dudman, I.P. Danks, C.D. Hall, J. Knychala and M.C. Grossel, J. Organomet. Chem., 306 (1986) 367.
3 I.P. Danks, Ph.D. Thesis, University of London, 1988.
4 C.D. Hall, N.W. Sharpe, I.P. Danks and Y.P. Sang, J. Chem. Soc. Chem. Commun., (1989) 419.
5 C.D. Hall, I.P. Danks, M.C. Lubienski and N.W. Sharpe, J. Organomet. Chem., 384 (1990) 139.
6 B.J. Hathaway, D.G. Holah and A.E. Underhill, J. Chem. Soc., (1962) 2444.
7 K.J. Johnson, Numerical Methods in Chemistry, Marcel Dekker, New York, 1980.
8 A.P. Bell and C.D. Hall, J. Chem. Soc. Chem. Commun., (1980) 163.
9 M. Hillman, B. Gordon, A.J. Weiss and A.P. Guzilkowski, J. Organomet. Chem., 155 (1978) 77.
10 M. Sato, S. Tanaka, S. Ebine, K. Morinaga and S. Akabori, J. Organomet. Chem., 282 (1985) 247.
11 T.H. Barr and W.E. Watts, Tetrahedron, 24 (1968) 6111.
12 P.D. Beer, C.D. Bush and T.A. Hamor, J. Organomet. Chem., 339 (1988) 133.
13 Y.S. Sohn, D.N. Hendrickson and H.B. Gray, J. Am. Chem. Soc., 93 (1971) 3603.
14 N. Rosch and K.H. Johnson, Chem. Phys. Lett., 24 (1974) 179.
15 M.C. Zerner, G.H. Loew, R.F. Kirchner and U.T. Mueller-Westerhoff, J. Am. Chem. Soc., 102 (1980) 589.